A paradigm shift on stabilising NTMs

Or: How I learned to stop worrying and love the Locked Mode

Richard Nies, Allan H. Reiman, Nathaniel J. Fisch

Princeton Plasma Physics Laboratory, Princeton University

IAEA Technical Meeting on Plasma Disruptions and their Mitigation, 20-23 July 2020

Outline

- For disruption avoidance, magnetic island (e.g. NTM) stabilisation is crucial. 95% of disruptions in JET with ILW are preceded by locked islands [1].

- New insights challenge rotating island stabilisation strategy.

- The case for locked mode stabilisation: more efficient & less sensitive to misalignment, broadening, large w_{seed}, time delay… ⇒ reduced power and increased robustness.

[1] Gerasimov et al. 2018

New challenges for rotating island stabilisation

- Low rotation in ITER ($f_{2/1} \sim 0.42$ kHz) compared to medium-sized devices (10s of kHz), leads to fast locking.
  With blanket [2]: $t_{\mathrm{lock}} \sim 2.5$ s, $w_{\mathrm{lock}}/a \sim 5\,\%$, for $Z_{\mathrm{eff}} = 1$.
  For $Z_{\mathrm{eff}} \sim 1.5$, $t_{\mathrm{lock}} \sim 1.7$ s.

- Must reduce island width below $w_{\mathrm{crit}} \sim 4$ cm.

- Sensitive to broadening and misalignment. Broadening by 2.5-3.5 due to edge density fluctuations predicted for ITER [3].

- Current strategy: avoid locked modes at all cost. Is this the right approach?

[2] La Haye et al. 2017
[3] Snicker et al. 2018

How bad are LMs really?

Based on experience with large LMs, commonly stated reasons to avoid locking:

- *"Leads to disruptions"*: not for small $w_{\mathrm{lock}}/a \lesssim 5\,\%$

- *"Locking to error field makes them inaccessible to ECCD":* Stabilisation possible by using static external fields to lock island in front of ECCD, as demonstrated on DIII-D [4].

- *"Loss of rotation (and H-mode)"*: yes and no,

  - even for large w, time window $\sim \tau_M \approx \tau_E$ between locking and loss of H-mode (e.g. [5]). H-mode preserved if fast stabilisation after locking, even for large DIII-D island [6].

  - for small w, actually closer to benign LMs induced by ELM suppression RMPs? How bad can rotation braking be if we already have zero rotation at pedestal top?

[4] Volpe et al. 2015
[5] Nelson et al. 2017
[6] Volpe et al. 2017 (online presentation)

Geometry of Island stabilisation

Plot of local stabilisation efficiency η_{aux}

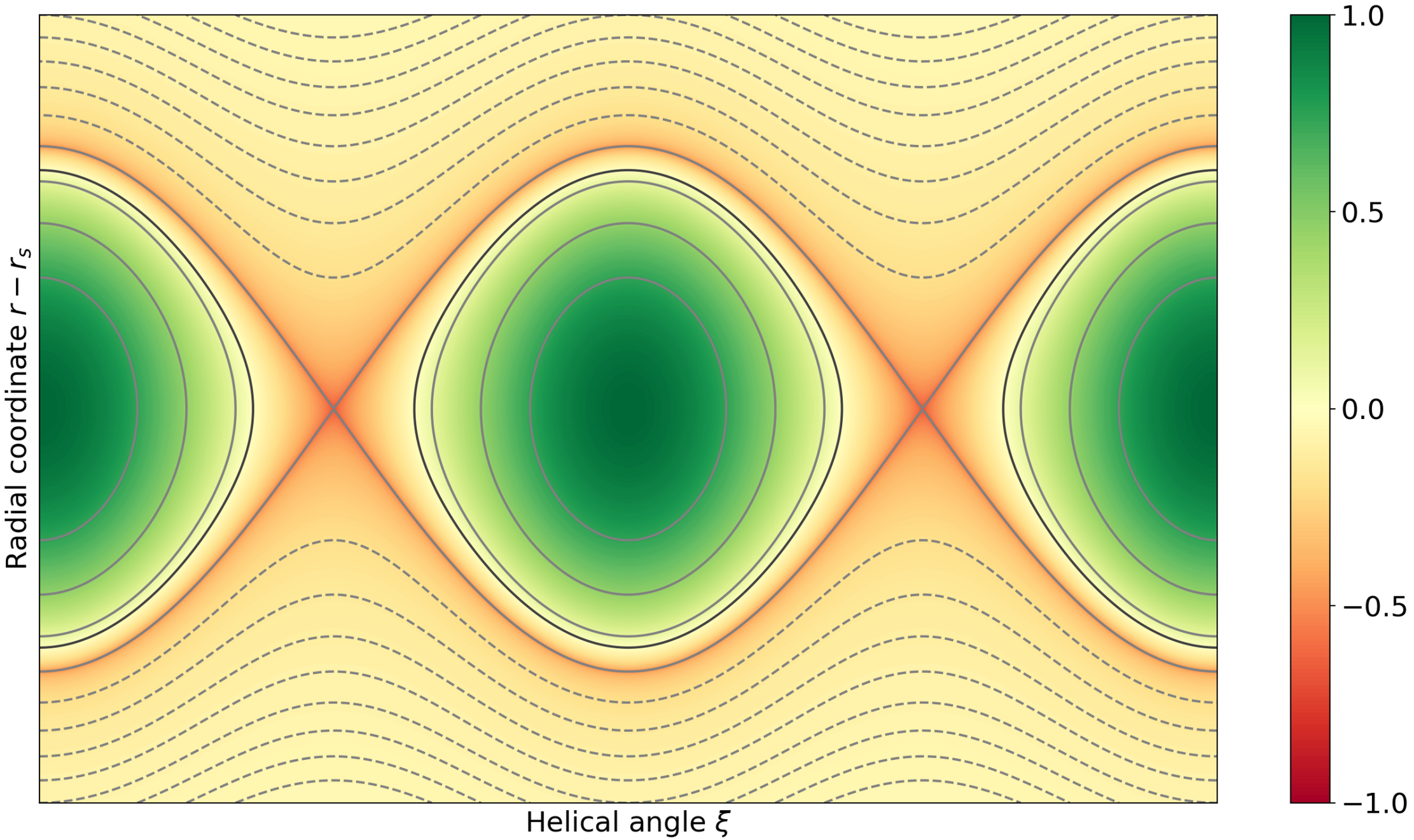

Rotating island, continuous ECCD

Average efficiency: $\langle \eta_{\mathrm{aux}} \rangle = 0.32$

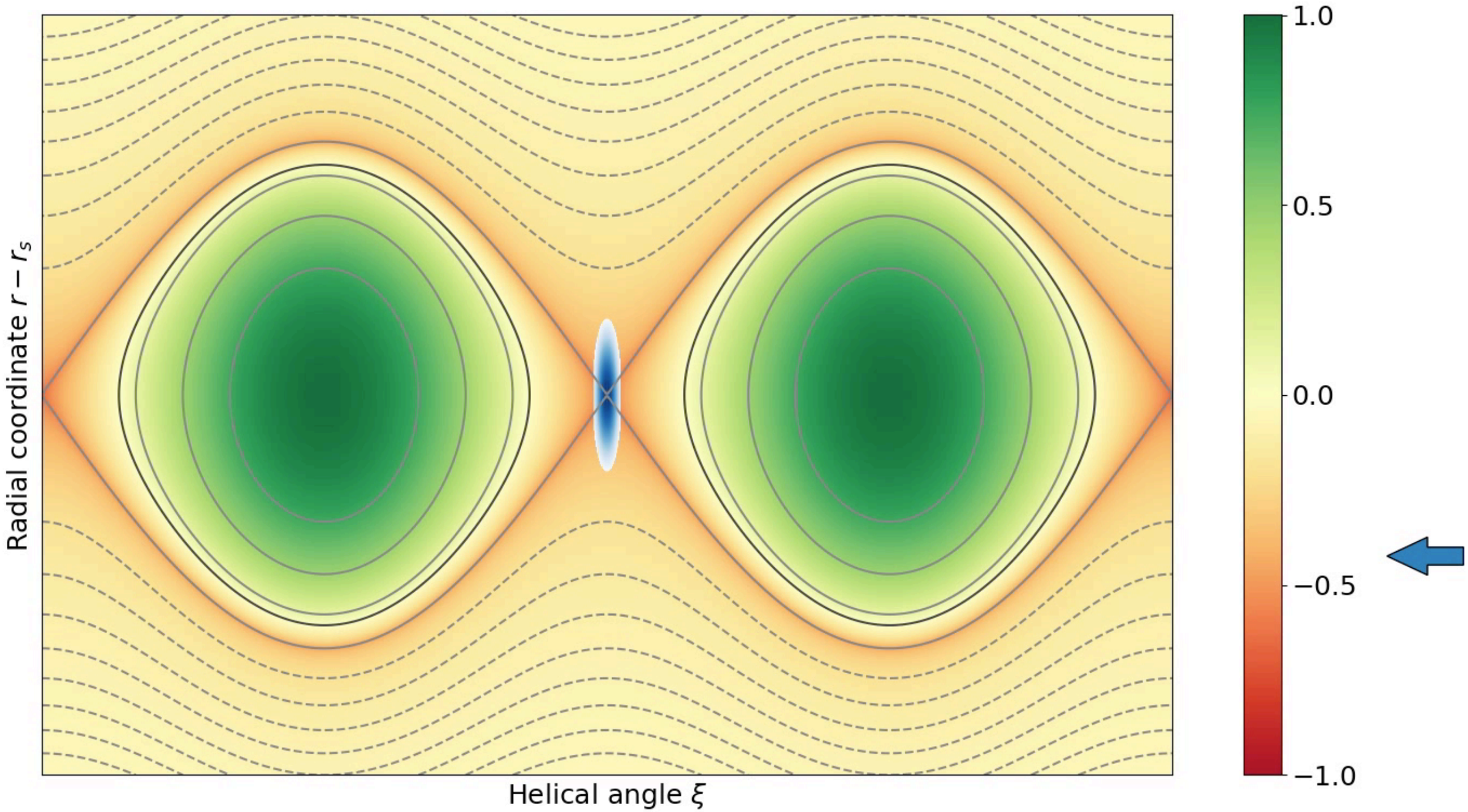

Rotating island, modulated ECCD

Average efficiency: $\langle \eta_{\mathrm{aux}} \rangle = 0.38$

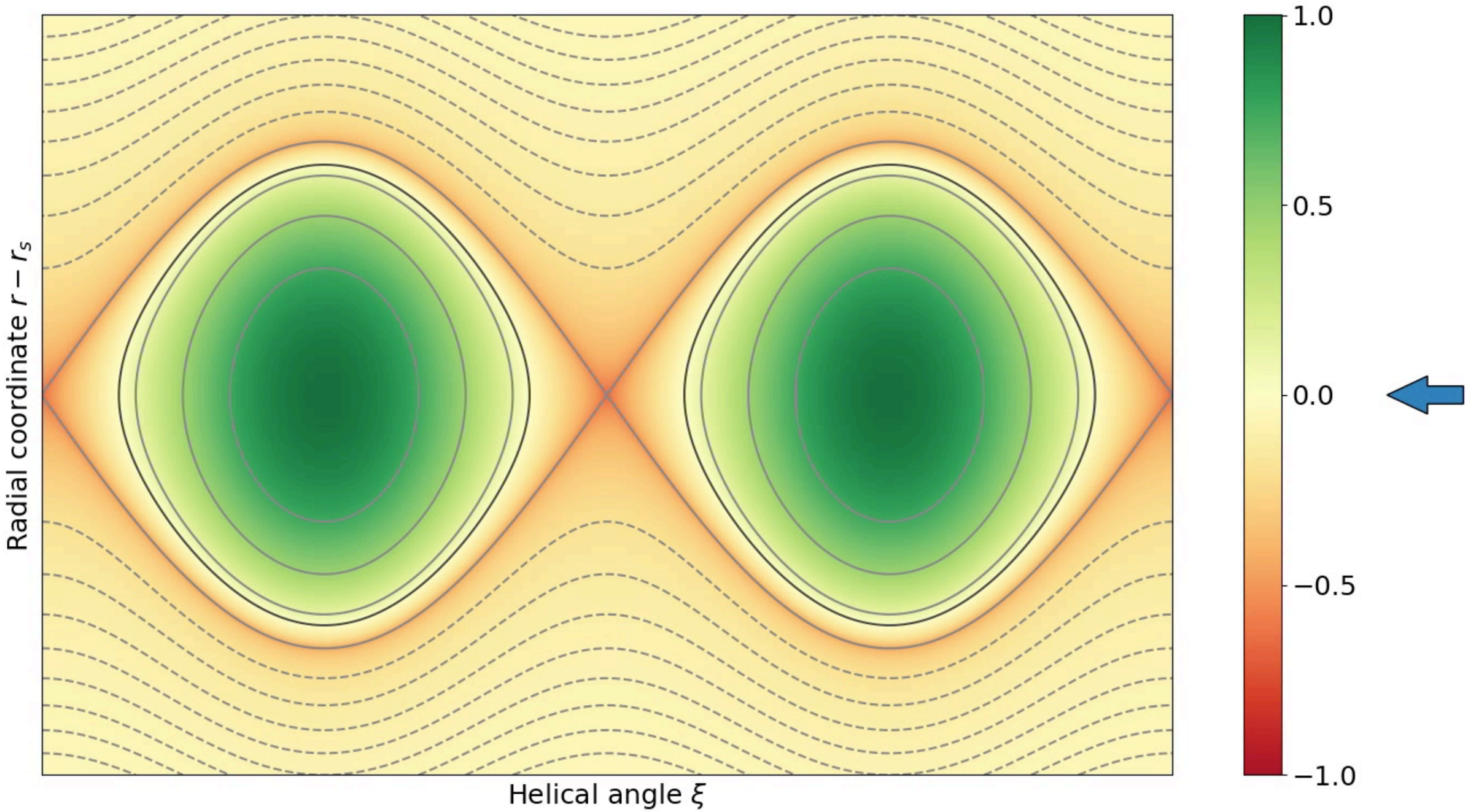

Geometric advantage of Locked Modes

Efficiency: $\eta_{\mathrm{aux}} = 0.95$

Higher efficiency.
+ larger radial width at O-point reduces sensitivity to misalignment and broadening

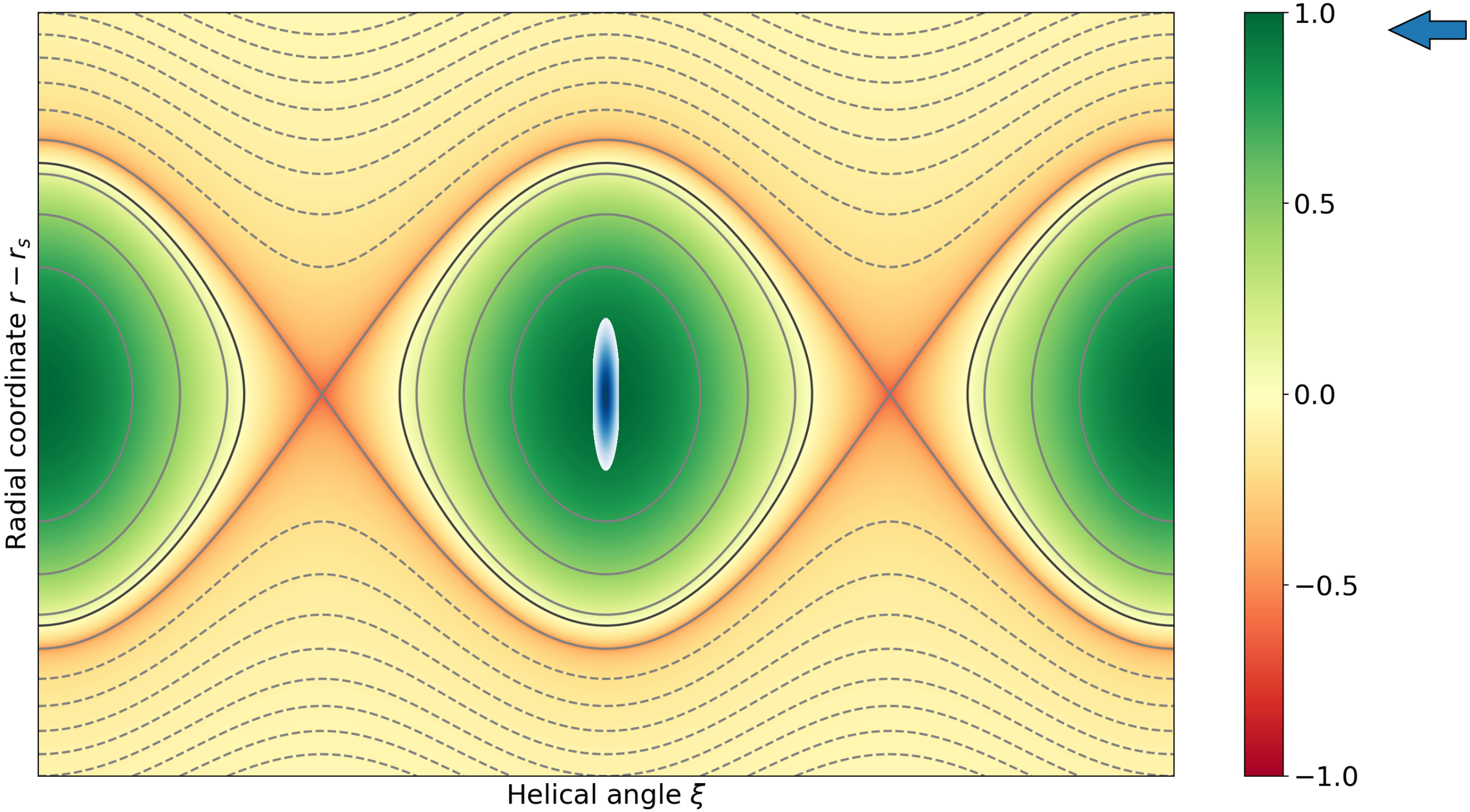

Island evolution equations

Generalised Rutherford Equation

$$0.82\frac{\tau_r}{r_s}\frac{\mathrm{d}w}{\mathrm{d}t} = \underbrace{r_s\left[\Delta'_0 - \Delta'_{0,\mathrm{wall}}(\omega)\right]}_{\text{Classical [2,7]}} + \underbrace{2m\left(\frac{w_{\mathrm{vac}}}{w}\right)^2\cos(\phi-\phi_{\mathrm{EF}})}_{\text{Error field / RMP [8]}} + a_2\frac{j_{\mathrm{BS}}}{j_{\parallel}}L_q\left(\underbrace{\frac{2}{3w}-\frac{3w_{\mathrm{ib}}^2}{w^3}}_{\text{Bootstrap and polarisation [2]}} - \underbrace{\frac{3\pi^{3/2}}{4w_{\mathrm{dep}}}\frac{w_{\mathrm{dep}}^2}{w^2}\eta_{\mathrm{NTM}}\eta_{\mathrm{aux}}}_{\text{Current drive [9]}}\right)$$

Equation of angular motion

$$\frac{\mathrm{d}\omega}{\mathrm{d}t} = \underbrace{\frac{\omega_0(\tau_M/\tau_{M0})-\omega}{\tau_M}}_{\text{Viscous [2]}} - \frac{1}{\tau_{A0}^2}\left(\frac{w}{a}\right)^3\left[\underbrace{\frac{C_1}{m}\frac{\omega\tau_w}{(\omega\tau_w)^2+1}}_{\text{Resistive wall [2,7]}} + \underbrace{\frac{m^2}{256}\left(\frac{a}{L_q}\right)^2\left(\frac{w_{\mathrm{vac}}}{w}\right)^2\sin(\phi-\phi_{\mathrm{EF}})}_{\text{Error field / RMP [8]}}\right]$$

Extension of previous work in [2,10,11]

More details on each term
in Appendix

[2] La Haye et al. 2017
[7] Nave and Wesson 1990
[8] Fitzpatrick 1993
[9] De Lazzari and Westerhof 2009
[10] van den Brand et al. 2012
[11] La Haye et al. 2006

Island evolution in action

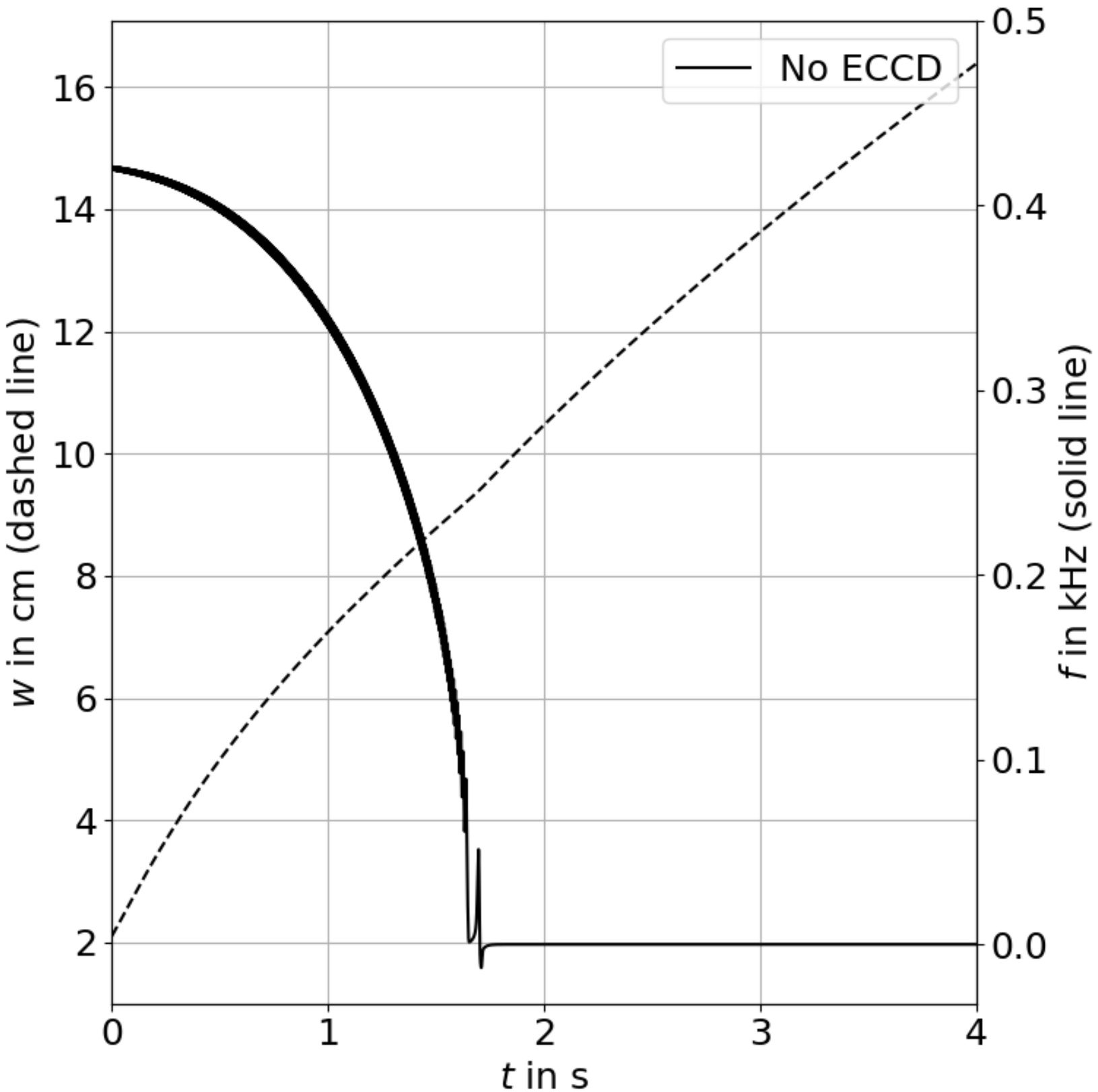

Base settings:

$w_{\mathrm{seed}} = 2.1$ cm

$w_{\mathrm{vac}} = 2.5$ cm

Island evolution in action

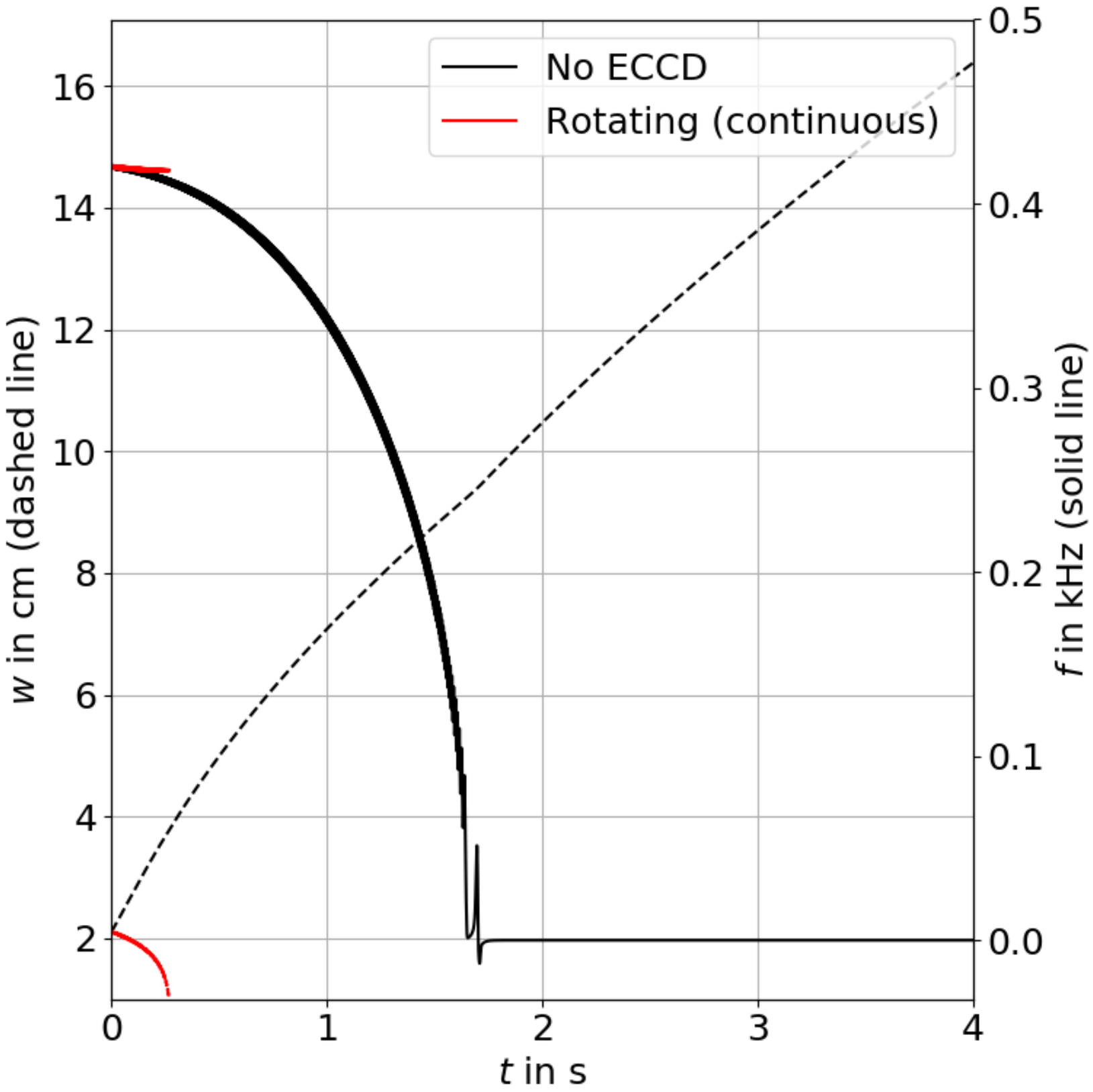

Base settings:

$w_{\mathrm{seed}} = 2.1$ cm

$w_{\mathrm{vac}} = 2.5$ cm

EC settings:

$w_{\mathrm{dep}} = 4$ cm

$x_{\mathrm{mis}} = 0$ cm

Continuous:

preemptive ($t_{\mathrm{delay}} = 0$)

$P_{\mathrm{EC}} = 6$ MW

Island evolution in action

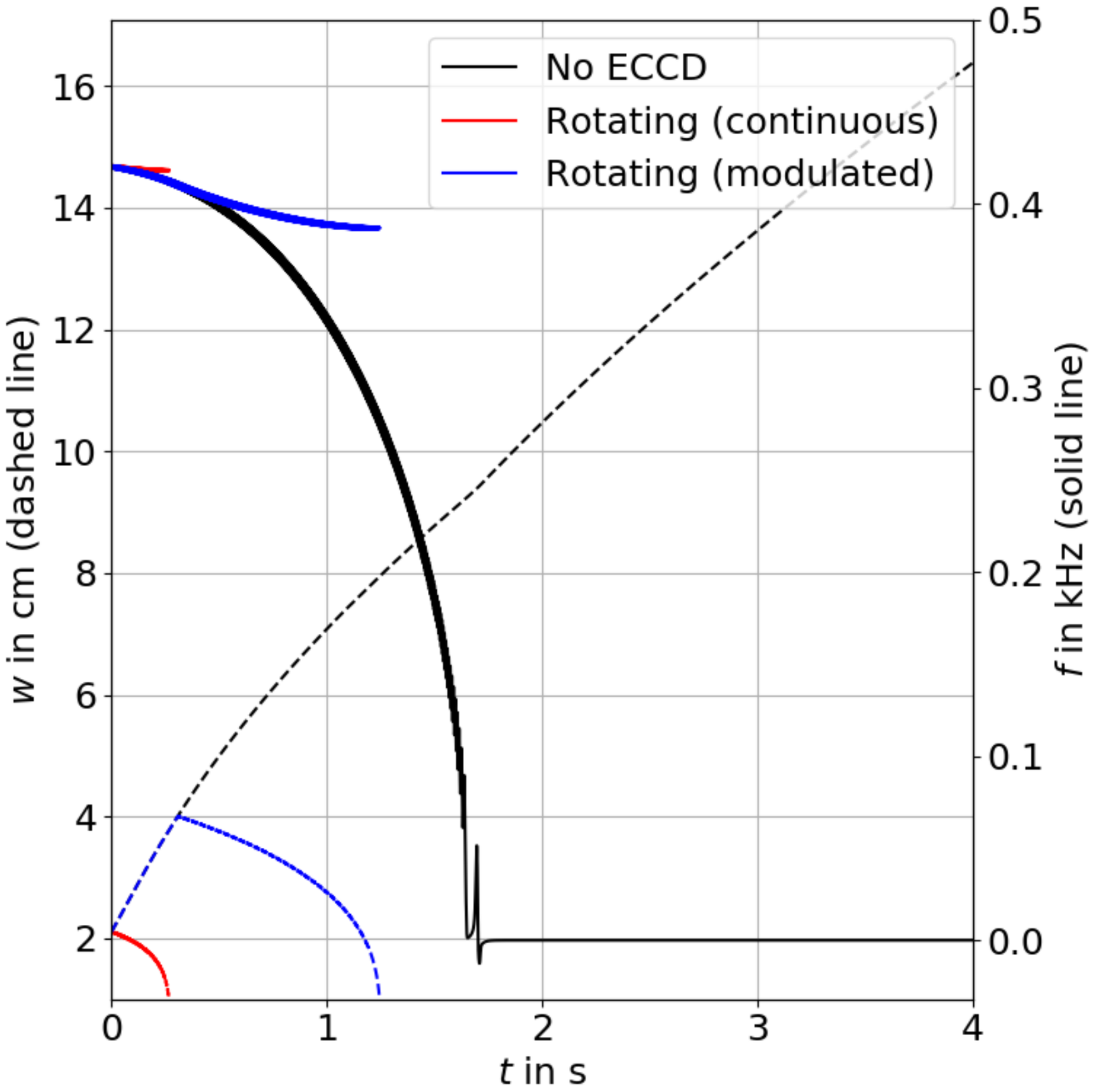

Base settings:

$w_{\mathrm{seed}} = 2.1$ cm

$w_{\mathrm{vac}} = 2.5$ cm

EC settings:

$w_{\mathrm{dep}} = 4$ cm

$x_{\mathrm{mis}} = 0$ cm

Continuous:

preemptive ($t_{\mathrm{delay}} = 0$)

$P_{\mathrm{EC}} = 6$ MW

Modulated (50%):

$w_{\mathrm{detect}} = 4$ cm

$P_{\mathrm{EC}} = 5$ MW

Island evolution in action

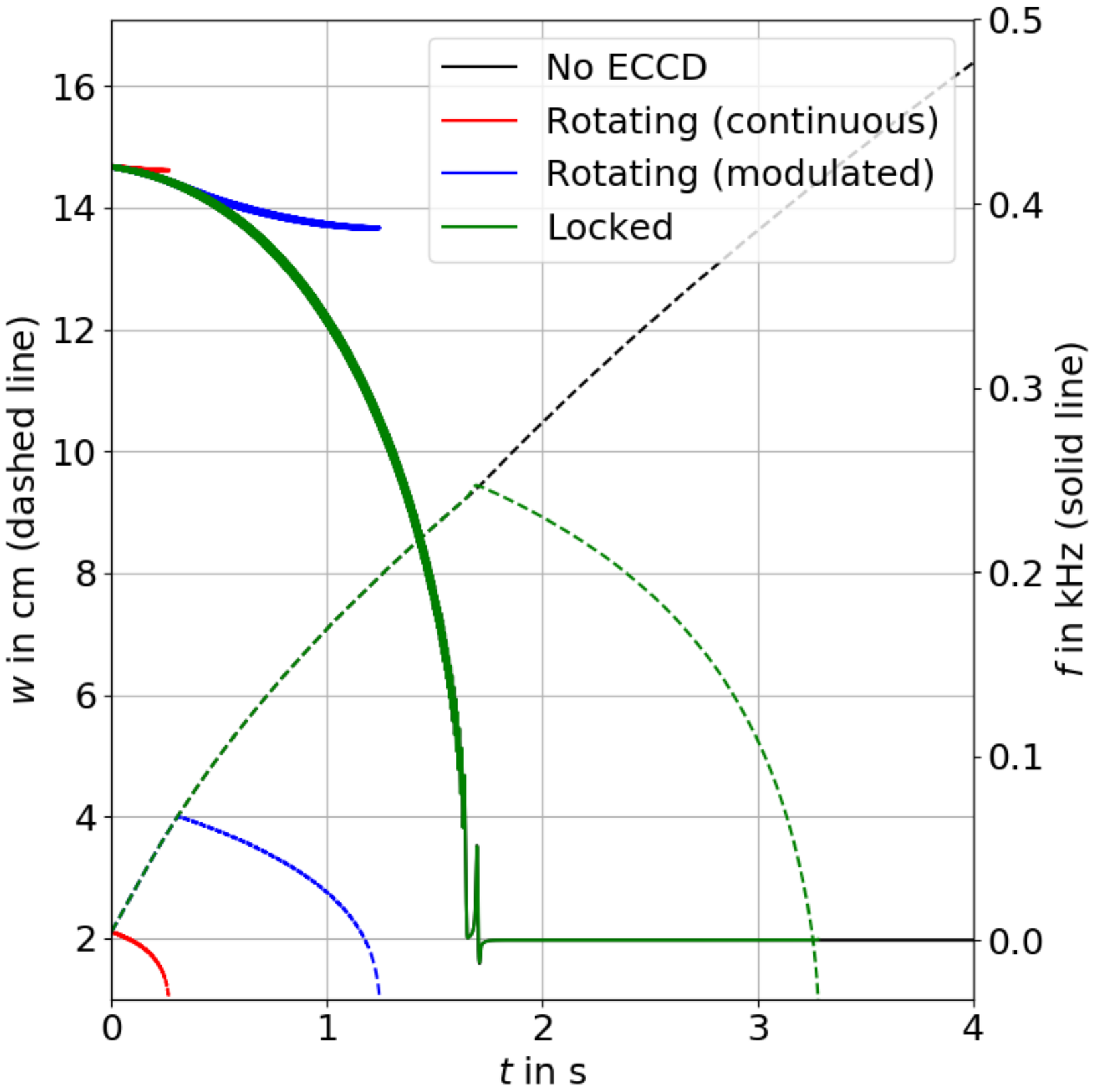

Base settings:

$w_{\mathrm{seed}} = 2.1$ cm

$w_{\mathrm{vac}} = 2.5$ cm

EC settings:

$w_{\mathrm{dep}} = 4$ cm

$x_{\mathrm{mis}} = 0$ cm

Continuous:

preemptive ($t_{\mathrm{delay}} = 0$)

$P_{\mathrm{EC}} = 6$ MW

Modulated (50%)**:**

$w_{\mathrm{detect}} = 4$ cm

$P_{\mathrm{EC}} = 5$ MW

Locked:

$P_{\mathrm{EC}} = 5$ MW

Main effects impacting power requirement

- Broadening: so far, $w_{\mathrm{dep}} = 4$ cm. Broadening by factor 2.5-3.5 due to edge density fluctuations [3].

- Radial misalignment: so far, $x_{\mathrm{mis}} = 0$. Consider $x_{\mathrm{mis}} \sim 1$ cm (e.g. due to inaccurate tracking, mirror sensitivity).

- NTM seeding: so far, $w_{\mathrm{seed}} \sim 2$ cm. Seeding up to $w \sim 5\,\% a = 10$ cm with sawteeth?

- Covered in appendix: w_{detect}, w_{vac}

[3] Snicker et al. 2018

Broadening

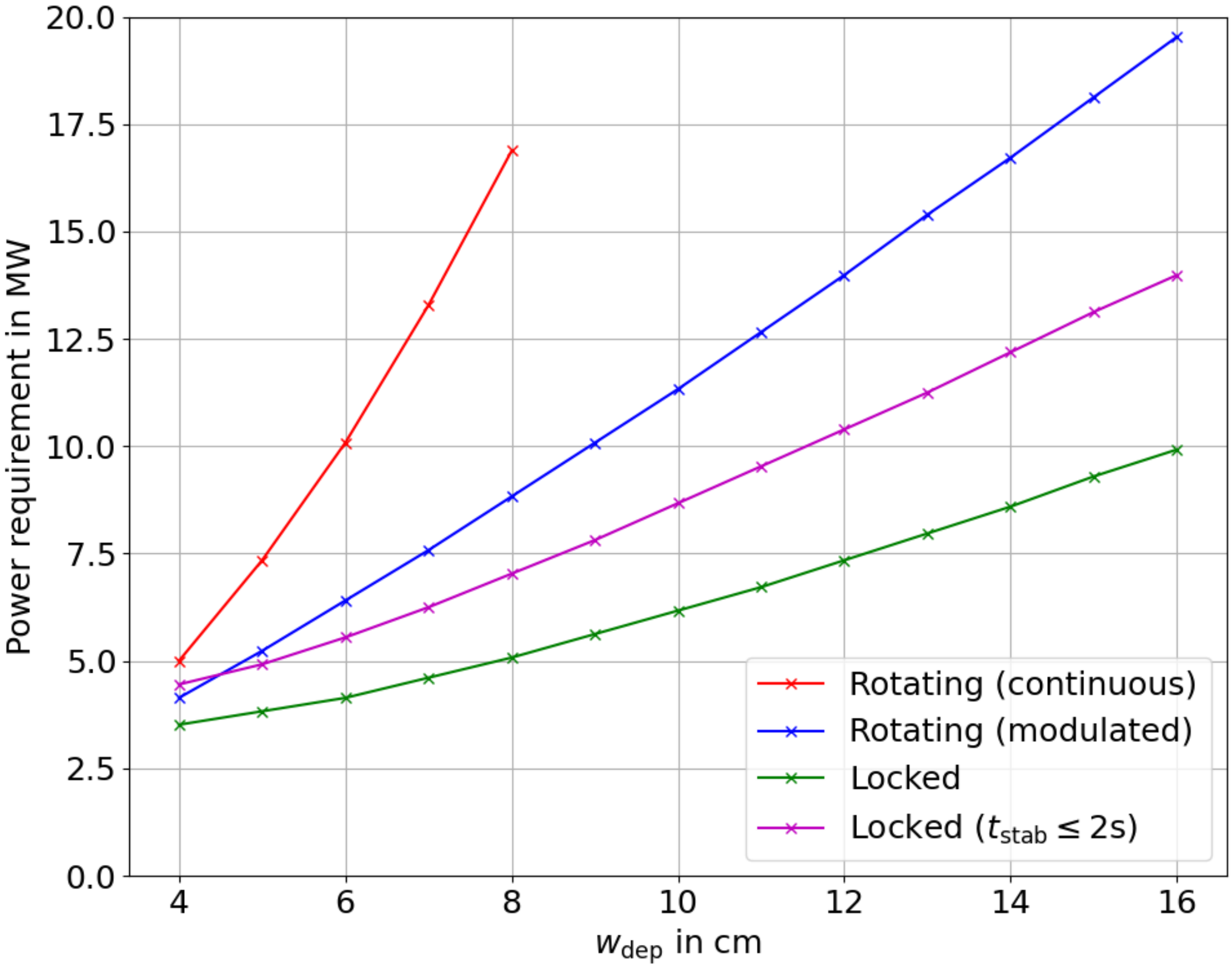

$w_{vac} = 2.5$ cm
$w_{seed} = 2.1$ cm
$x_{mis} = 0$ cm

Criterion for rotating island:
$w < 4$ cm

Misalignment

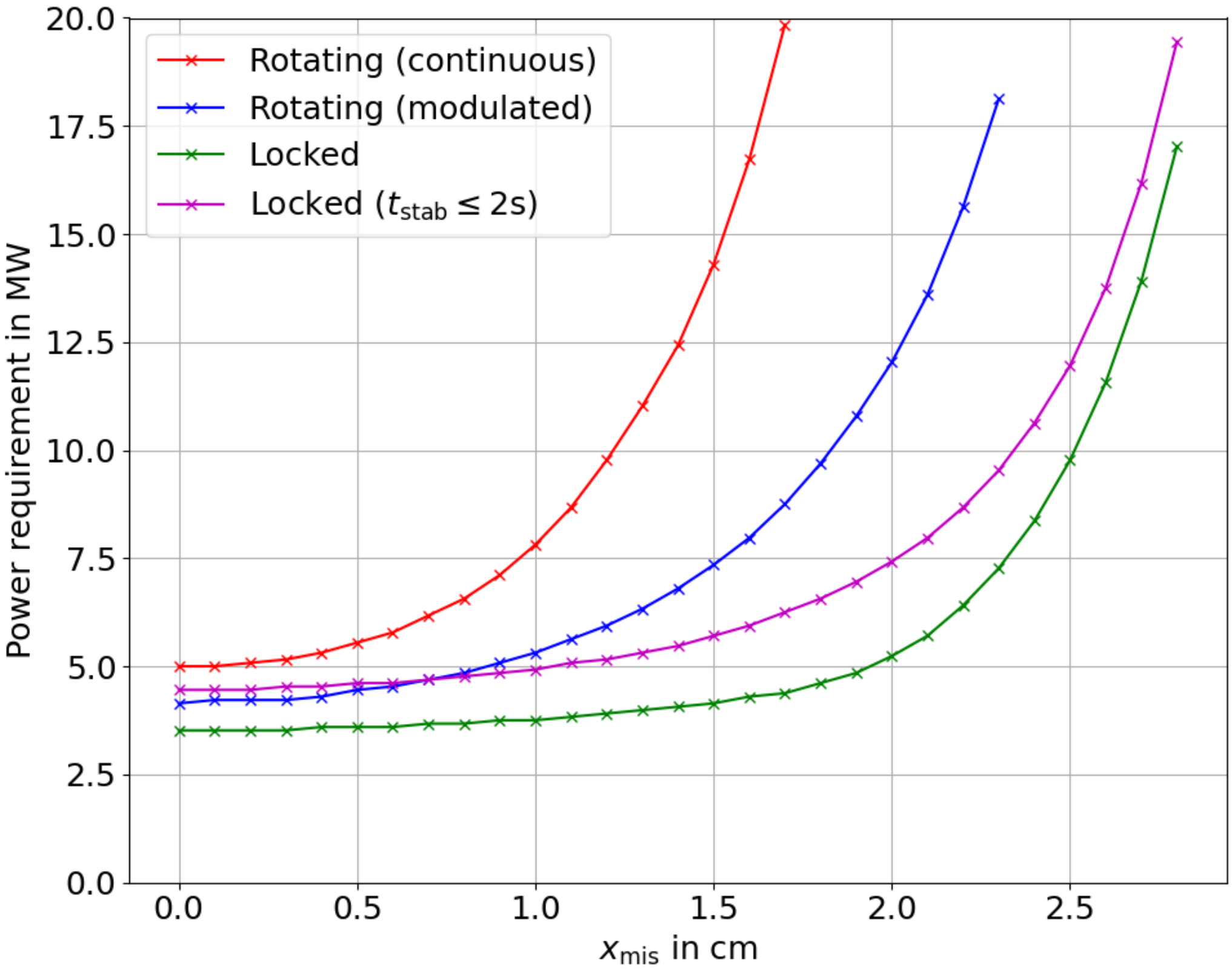

$w_{vac} = 2.5$ cm
$w_{seed} = 2.1$ cm
$w_{dep} = 4$ cm

Criterion for rotating island:
$w < 4$ cm

Seeding width

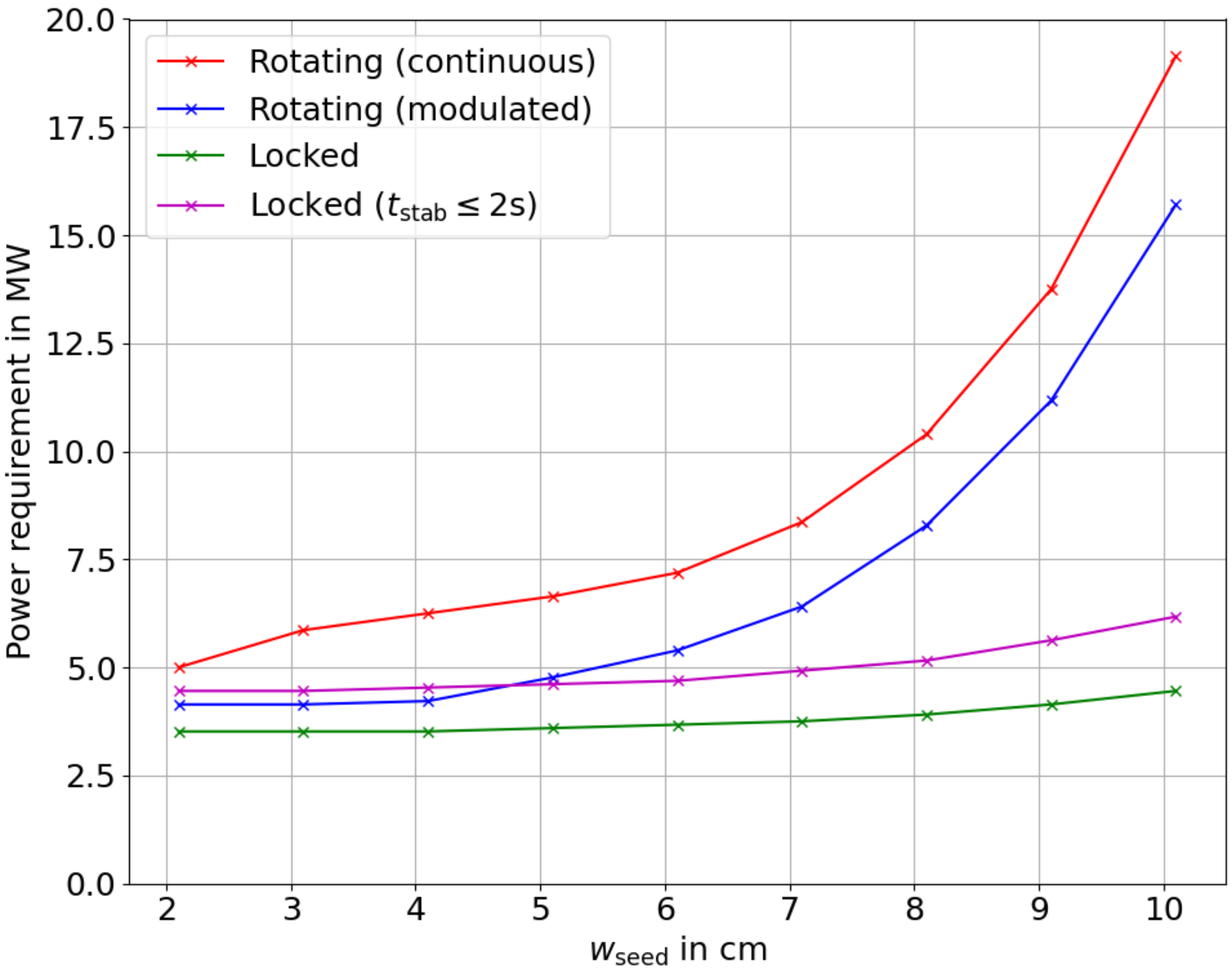

$w_{vac} = 2.5$ cm

$w_{dep} = 4$ cm

$x_{mis} = 0$ cm

Criterion for rotating island:

$w < 4$ cm

Power requirement with all effects

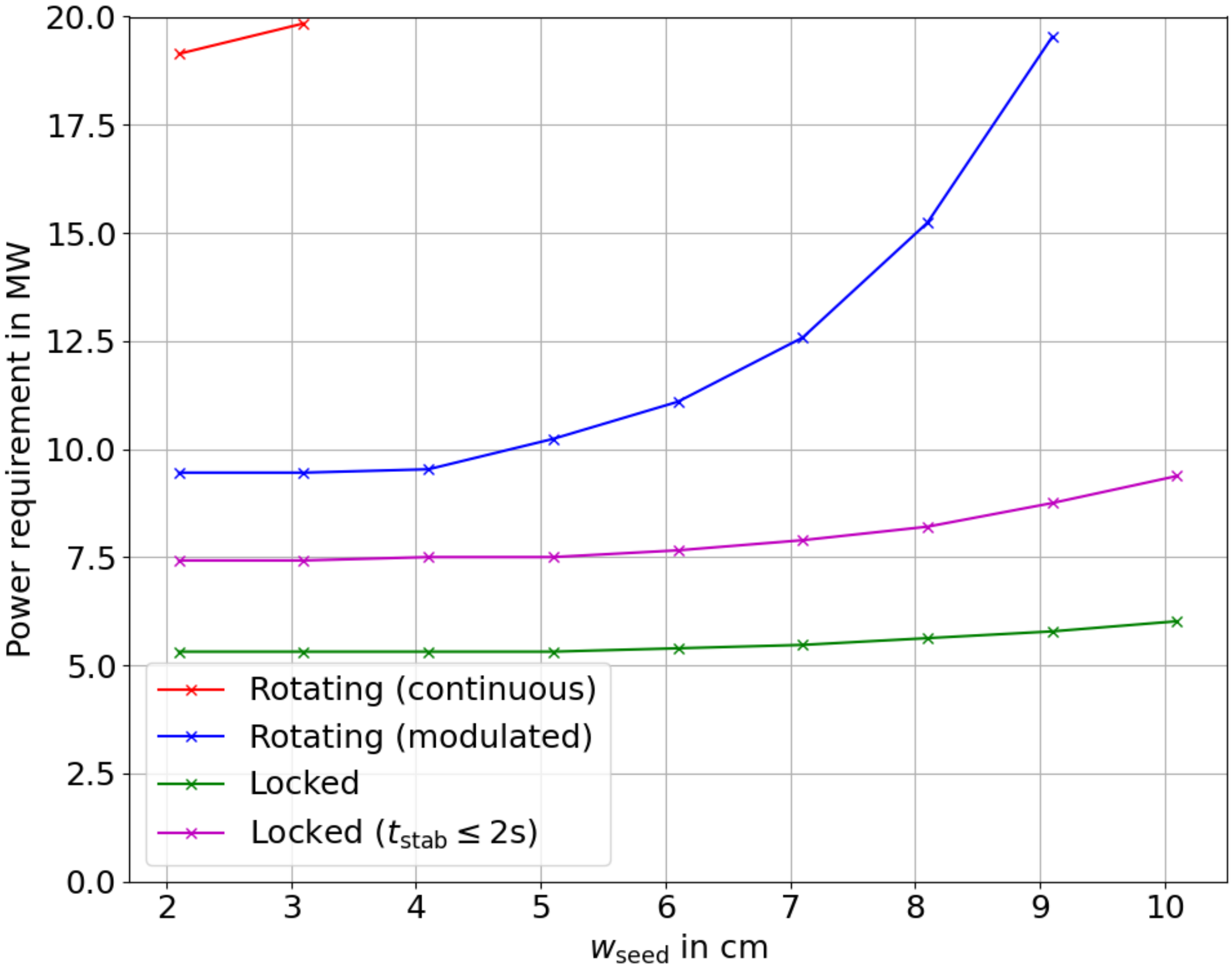

$w_{\mathrm{vac}} = 2.5$ cm

$w_{\mathrm{dep}} = 8$ cm

$x_{\mathrm{mis}} = 1$ cm

Criterion for rotating island:

$w < 4$ cm

Summary and next steps

- Advantages of LM stabilisation: dynamical (fast locking ⇒ rotating island stabilisation is hard + w_{lock} is small) and geometrical (higher stabilisation efficiency, less sensitive to misalignment and broadening).

- Stabilisation of small LMs is efficient (lower EC power) and robust (no problem with large w_{seed}, detection threshold).

- A lot of attention on rotating island stabilisation, comparatively little for locked modes [4, 5, 12]. Let us correct that.

- Open questions: are small LMs a problem for confinement? Optimisation for ITER and beyond - launching angles, combined strategies, low rotation scenarios, …? Importance of current condensation (See also presentation by A.H. Reiman)? How reliable for disruption avoidance in experiment?

[4] Volpe et al. 2015
[5] Nelson et al. 2020
[12] Yu and Guenter 2008

Thank you!

Questions and feedback are welcome

References

[1] Gerasimov, S. N. et al. Overview of disruptions with JET-ILW. in 27th IAEA Fusion Energy Conference (FEC 2018) (2018)

[2] La Haye, R. J., Paz-Soldan, C. & Liu, Y. Q. Effect of thick blanket modules on neoclassical tearing mode locking in ITER. *Nucl. Fusion* **57**, 014004 (2017).

[3] Snicker, A. *et al.* The effect of density fluctuations on electron cyclotron beam broadening and implications for ITER. *Nucl. Fusion* **58**, 016002 (2018).

[4] Volpe, F. A. *et al.* Avoiding Tokamak Disruptions by Applying Static Magnetic Fields That Align Locked Modes with Stabilizing Wave-Driven Currents. *Physical Review Letters* **115**, (2015).

[5] Nelson, A.O. *et al.* Experimental evidence of ECCD-based NTM suppression threshold reduction during mode locking on DIII-D. *Plasma Phys. Control. Fusion* **in press,** (2020)

[6] F. Volpe, presentation at ITER Summer School on Disruption Physics and Control, (2017)

[7] Nave, M. F. F. & Wesson, J. A. Mode locking in tokamaks. *Nucl. Fusion* **30**, 2575–2583 (1990).

[8] Fitzpatrick, R. Interaction of tearing modes with external structures in cylindrical geometry (plasma). *Nucl. Fusion* **33**, 1049–1084 (1993).

[9] De Lazzari, D. & Westerhof, E. On the merits of heating and current drive for tearing mode stabilization. *Nuclear Fusion* **49**, 075002 (2009).

[10] van den Brand, H., de Baar, M. R., Cardozo, N. J. L. & Westerhof, E. Integrated modelling of island growth, stabilization and mode locking: consequences for NTM control on ITER. *Plasma Phys. Control. Fusion* **54**, 094003 (2012).

[11] Haye, R. J. L. *et al.* Cross–machine benchmarking for ITER of neoclassical tearing mode stabilization by electron cyclotron current drive. *Nucl. Fusion* **46**, 451–461 (2006).

[12] Yu, Q. & Günter, S. Locking of neoclassical tearing modes by error fields and its stabilization by RF current. *Nucl. Fusion* **48**, 065004 (2008).

[13] Polevoi, *private comm.* (2019)

[14] Hender, T. C. *et al.* Chapter 3: MHD stability, operational limits and disruptions. *Nucl. Fusion* **47**, S128–S202 (2007).

[15] Glasser, A. H., Greene, J. M. & Johnson, J. L. Resistive instabilities in general toroidal plasma configurations. *The Physics of Fluids* **18**, 875–888 (1975).

[16] Fitzpatrick, R. Helical temperature perturbations associated with tearing modes in tokamak plasmas. *Physics of Plasmas* **2**, 825–838 (1995).

Supplementary Material

Appendix 1:

Glossary of quantities and values

Values used in simulations (mostly from [2])

Resistive time: $\tau_R = \mu_0 r_s^2 \eta^{-1}$

Radius of $q = 2$ surface: $r_s = 155$ cm

Resistivity:
$\eta^{-1} = 1258 (T_e / 1\ \text{eV})^{3/2} f_\epsilon / Z_{\text{eff}}$

Electron temperature: $T_e = 5.63$ keV

Trapped particle fraction: $f_\epsilon = 0.26$

Effective ion charge [13]: $Z_{\text{eff}} = 1.53$

Shear length: $L_q = 94$ cm

Bootstrap current: $j_{\text{BS}} = 7.2 \cdot 10^4$ A/m^2

Average parallel current:
$j_\parallel = 38.8 \cdot 10^4$ A/m^2

Radius of resistive wall: $r_w = 1.25\ a$

Resistive wall time: $\tau_w = 14$ ms

Alfven time: $\tau_{A0} = 3\ \mu$s

Original rotation frequency:
$\omega_0 = 2\pi \cdot 0.42$ kHz

Original momentum confinement time:
$\tau_{M0} = 3.7$ s

Fitting coefficients:
$C_1 = 1/80, \quad C_M = 12$

Appendix 2:

Rutherford equation term by term

Classical tearing index Δ'_0

The classical tearing mode contribution is given by the jump in the derivative of the magnetic perturbation ψ at the rational surface r_s:

$$r_s\Delta'_0 = \frac{\frac{\partial\psi}{\partial r}(r_s^+) - \frac{\partial\psi}{\partial r}(r_s^-)}{\psi(r_s)}.$$

For a fast rotating island, the resistive wall acts like a perfect conductor, thus giving an additional stabilising contribution which can be approximated as [8]

$$r_s\Delta'_{\text{wall}} = -2m\left(\frac{r_s^+}{r_w}\right)^{2m} \frac{(\omega\tau_w)^2\left[1-\left(\frac{r_s^+}{r_w}\right)^{2m}\right]}{1+(\omega\tau_w)^2\left[1-\left(\frac{r_s^+}{r_w}\right)^{2m}\right]^2},$$

where r_w is the wall radius, τ_w the resistive wall time and ω the island rotation frequency.

In our calculations, we assume $r_s\Delta'_0 = 1.71 + r_s\Delta'_{\text{wall}}$, such that $r_s\Delta'_0 = 1.1$ for the fast rotating island, as in [2].

Error field or RMP Δ'_{EF}

The error field or RMP term is given by [8]

$$r_s \Delta'_{\mathrm{EF,RMP}} = 2m \left(\frac{w_{\mathrm{vac}}}{w} \right)^2 \cos(\phi - \phi_{\mathrm{EF}}),$$

The vacuum island width is obtained from the magnetic field perturbation at the edge [8], which can be related to the radial error field at the plasma edge $b_{\mathrm{rn}} = B_r/B_t = m\psi(a)a$ [14], such that

$$w_{\mathrm{vac}} = 4a\sqrt{b_{\mathrm{rn}} \frac{B_t}{mB_p} \frac{L_q}{a} \left(\frac{r_s}{a} \right)^m} = \sqrt{\frac{b_{\mathrm{rn}}}{10^{-5}}} \cdot 2.2 \text{ cm}$$

To avoid error field penetration, ITER has a 3-field requirement

$$B_{3-\mathrm{mode}} = \sqrt{B_{2,1}^2 + 0.8B_{3,1}^2 + 0.2B_{r1,1}^2} \leq 5 \cdot 10^{-5} B_t \,.$$

It thus makes sense to take $w_{\mathrm{vac}} \sim 2.5 - 5.0$ cm.

Bootstrap Δ'_{BS}

The bootstrap term is modeled as [2, 11]

$$r_s \Delta'_{\mathrm{BS}} = \left(a_2 \frac{j_{\mathrm{BS}}}{j_{\parallel}} L_q \right) \frac{2}{3w},$$

where $a_2 = 2.8$ is a parameter fitted from experiment [11] to include toroidal effects in the bootstrap term, whereas $a = 4$ for a cylinder, so toroidal effects slightly reduce the magnitude of the bootstrap term. Furthermore, the factor $2/3$ originates from an additional stabilising Glasser-Greene-Johnson [15] contribution, obtained by experimental fit [2].

Note that, for consistency with [2,11], no incomplete pressure flattening term was included here, which would modify the bootstrap term at small island width as [16]

$$\frac{1}{w} \rightarrow \frac{w}{w^2 + w_{\mathrm{tra}}^2}.$$

Polarisation current Δ'_{pol}

The polarisation current is modeled as [2]

$$r_s \Delta'_{\mathrm{pol}} = -\left(a_2 \frac{j_{\mathrm{BS}}}{j_{\parallel}} L_q \right) \frac{3 w_{\mathrm{ib}}^2}{w^3},$$

with the ion banana width $w_{\mathrm{ib}} \sim \epsilon^{1/2} \rho_{\theta,i} \approx 0.7\ \mathrm{cm}$.

The term stabilises the island at small widths. The combination of bootstrap and polarisation current terms is negative (stabilising) for $w < 3 w_{\mathrm{ib}}/\sqrt{2} \sim 2.1 w_{\mathrm{ib}}$ and maximal for $w = \sqrt{3/2} \cdot 3 w_{\mathrm{ib}} \sim 3.7 w_{\mathrm{ib}}$.

Current drive Δ'_{CD} (1/2)

The current drive term is modeled as [9]

$$r_s \Delta'_{\mathrm{CD}} = -\left(a_2 \frac{j_{\mathrm{BS}}}{j_{\parallel}} L_q\right) \frac{3\pi^{3/2}}{4 w_{\mathrm{dep}}} \frac{w_{\mathrm{dep}}^2}{w^2} \eta_{\mathrm{NTM}} \eta_{\mathrm{aux}},$$

where w_{dep} is the $1/e$ width of the gaussian deposition and $\eta_{\mathrm{NTM}} = j_{\mathrm{CD,max}}/j_{\mathrm{BS}}$. The peak driven current $j_{\mathrm{CD,max}} = P_{\mathrm{tot}} \gamma_{\mathrm{CD}}$, with the quantity $\gamma_{\mathrm{CD}} = j_{\mathrm{CD,max}}/P_{\mathrm{tot}} \propto (I_{\mathrm{CD}}/w_{\mathrm{dep}})/P_{\mathrm{tot}}$ a measure of the current drive efficiency. The quantity $I_{\mathrm{CD}}/P_{\mathrm{tot}}$ is approximately constant for a given launching angle. We thus take $\gamma_{\mathrm{CD}} = 1.32 \cdot 10^{-4}\ (4\ \mathrm{cm}/w_{\mathrm{dep}})$ to match the value in [10] for a deposition width of $4\ \mathrm{cm}$ and appropriately decrease the peak current density when including broadening effects. Broadening leaves P_{tot} unchanged, but reduces $j_{\mathrm{CD,max}}$, so γ_{CD} must also be reduced accordingly.

Current drive Δ'_{CD} (2/2)

The stabilisation efficiency is given by [9]

$$\eta_{\mathrm{aux}} = \frac{\int_{-1}^{\infty} \mathrm{d}\Omega \, \langle p_{\mathrm{EC}} \rangle \frac{\langle \cos(m\xi) \rangle}{\langle 1 \rangle}}{\int_{-1}^{\infty} \mathrm{d}\Omega \, \langle p_{\mathrm{EC}} \rangle},$$

where $\Omega = 8x^2/w^2 - \cos(m\xi)$ is a flux coordinate ($\Omega = -1$ at the island O-point and $\Omega = 1$ at the separatrix), $\xi = \theta - n/m\phi$ a helical angle and angular brackets indicate flux surface averages. The power deposition is a gaussian in the radial direction and a delta function in the helical angle,

$$p_{\mathrm{EC}} \propto \exp\left(-4(x - x_{\mathrm{dep}})^2/w_{\mathrm{dep}}^2\right) \delta(m\xi - \phi + \phi_{\mathrm{EC}}).$$

The stabilisation efficiency is evaluated instantaneously as the phase evolves, even for the rotating island. Note in particular that no fast rotation needs to be assumed for the rotating island case, and that no arithmetic approximations to the stabilisation efficiency are used.

Appendix 3:

Equation of angular motion term by term

Viscous torque T_{visc}

The viscous torque is modeled as [2]

$$\dot{\omega}_{\text{visc}} = \frac{\omega_0(\tau_M/\tau_{M0}) - \omega}{\tau_M},$$

where $\tau_{M0} = 3.7\ \text{s}$ is the momentum confinement time without island, and $\tau_M = \tau_{M0}/(1 + C_M w/a)$ takes into account the confinement degradation due to the island's presence, with $C_M = 12$ fitted to a DIII-D IBS shot [2]. The original rotation frequency $\omega_0 = 2\pi f_0$, with $f_0 = 0.42\ \text{kHz}$.

The viscous torque tries to restore the island rotation to the background plasma rotation.

Resistive wall torque T_{wall}

The resistive wall torque is modeled as [2,7]

$$\dot{\omega}_{\text{wall}} = -\frac{1}{\tau_{A0}^2}\left(\frac{w}{a}\right)^3 \frac{C_1}{m}\frac{\omega\tau_w}{(\omega\tau_w)^2+1},$$

where $\tau_{A0} = 3.0\ \mu s$ is an Alfven time, $\tau_w = 14\ \text{ms}$ is the wall time of ITER's blanket and $C_1 = 1/80$ [2] (note there was a mistake in the original paper incorrectly reporting $C_1 = 1/20$).

Note the w^3 dependence instead of the w^4 dependence in [7], which originates from taking the island inertia instead of that of the entire plasma, see [2,11].

The resistive wall torque is the main reason for the fast braking of the island. The balance with the viscous torque gives the critical island width, $w_{\text{crit}} \sim 4\ \text{cm}$ in ITER, above which there is no fast rotating steady-state solution to the equation of angular motion, i.e. the island is on course for locking.

Error field / RMP torque $T_{\mathrm{EF/RMP}}$

The error field torque is modeled as [8]

$$\dot{\omega}_{\mathrm{EF/RMP}} = -\frac{1}{\tau_{A0}^2}\left(\frac{w}{a}\right)^3 \frac{m^2}{256}\left(\frac{a}{L_q}\right)^2\left(\frac{w_{\mathrm{vac}}}{w}\right)^2 \sin(\phi - \phi_{\mathrm{EF}}),$$

where the original formula from [8] was modified to take the island inertia instead of that of the entire plasma (see previous page and [2,11]).

If the rotation frequency is seen as a ball, the error field torque is like a hill. Once the ball is trapped in the hill, it is generally quickly decelerated and finally trapped at a phase close to the error field phase (depending on the relative strength of error field and viscous torques).

Example without ECCD

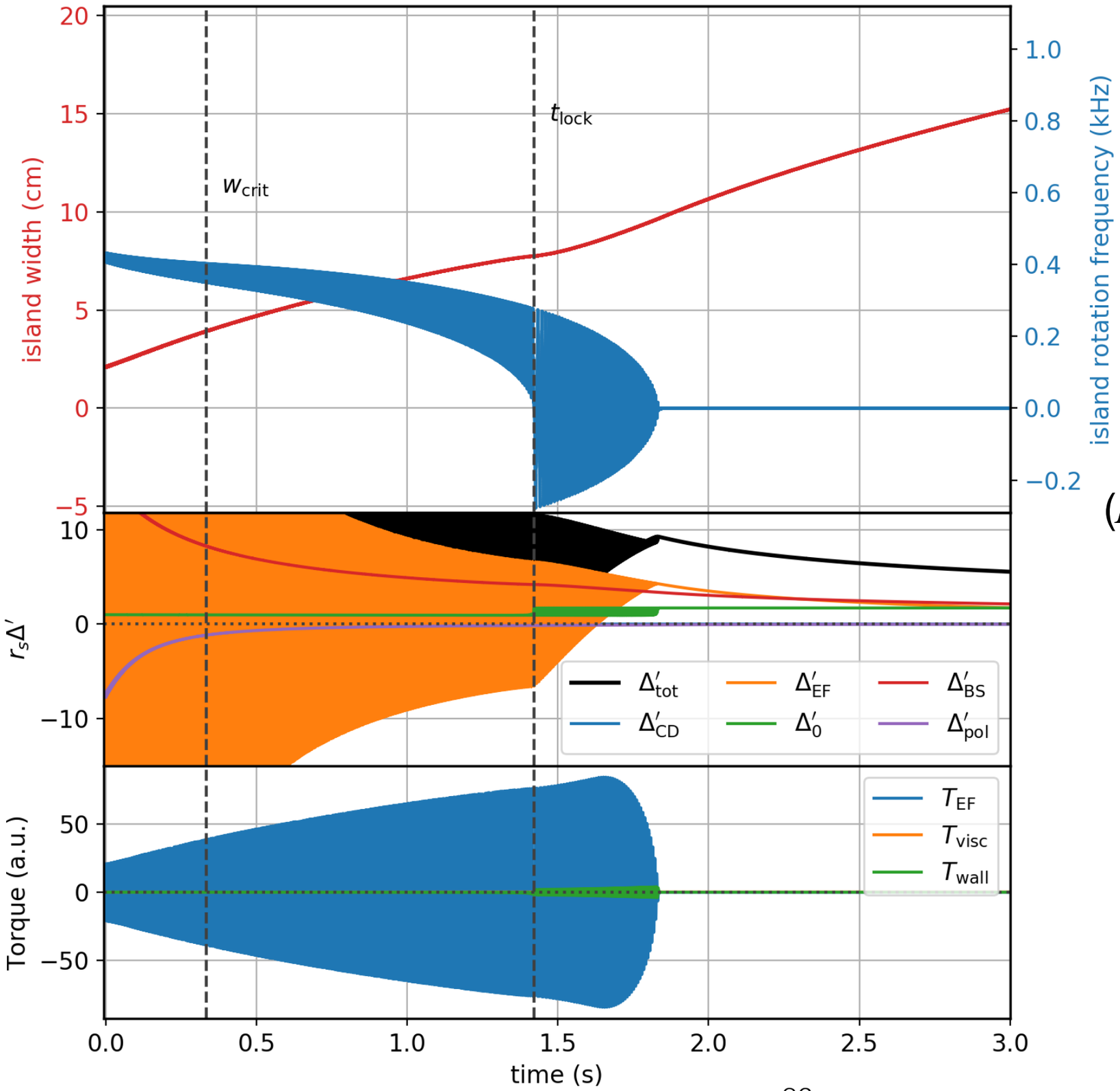

here, large $w_{\mathrm{vac}} = 10$ cm,
$(B_{\mathrm{r}}(a) \sim 2 \cdot 10^{-4} B_{\phi} \sim 10\ \mathrm{G})$

locking at $\phi \approx \phi_{\mathrm{EF}}$

driven reconnection
after locking

Appendix 4:

Different scenarios

(detection threshold, error field, …)

Power requirement with higher w_{vac}

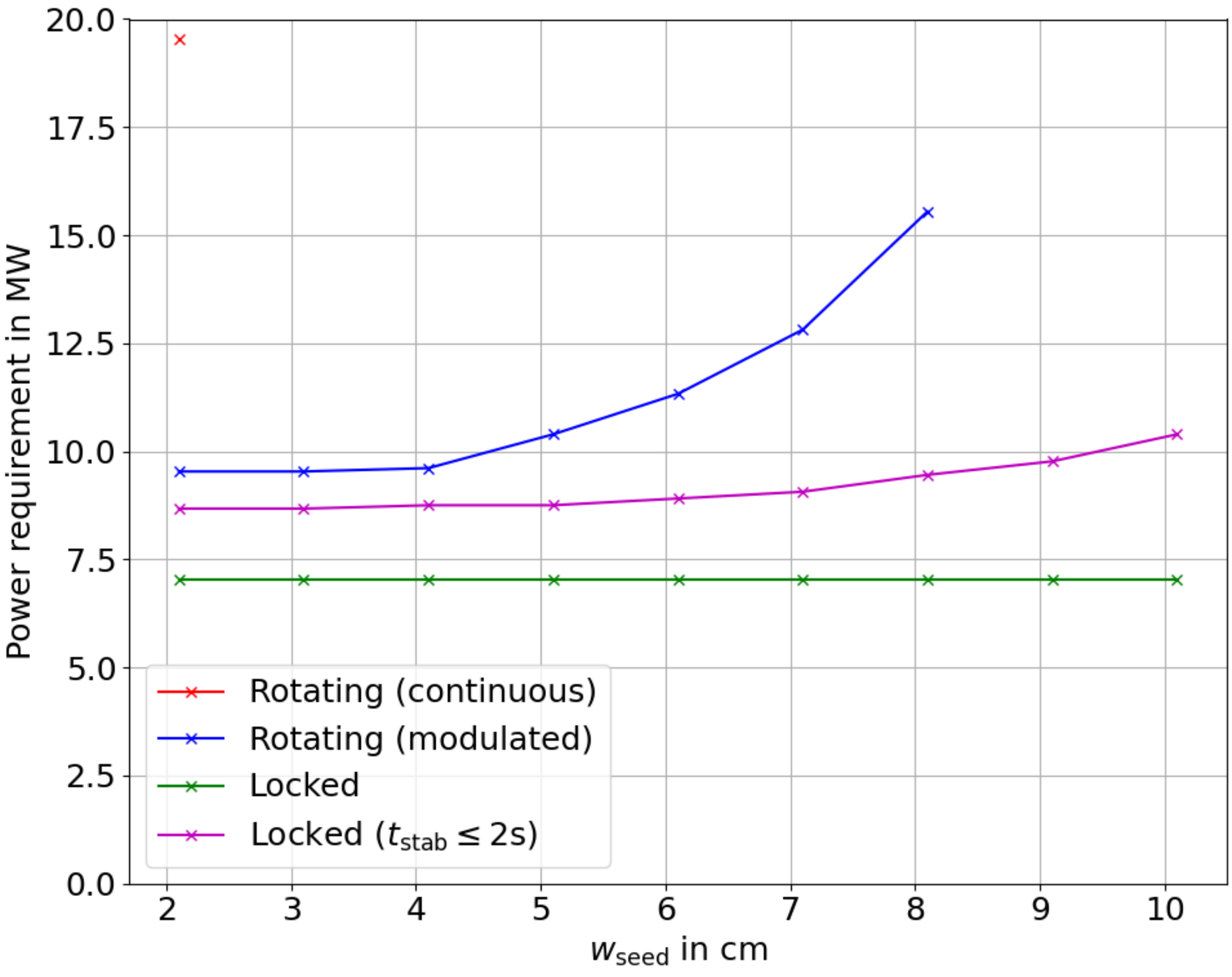

$w_{\mathrm{vac}} = 5$ cm

$w_{\mathrm{dep}} = 8$ cm

$x_{\mathrm{mis}} = 1$ cm

Criterion for rotating island:

$w < 4$ cm

Power requirement with higher w_{dep}

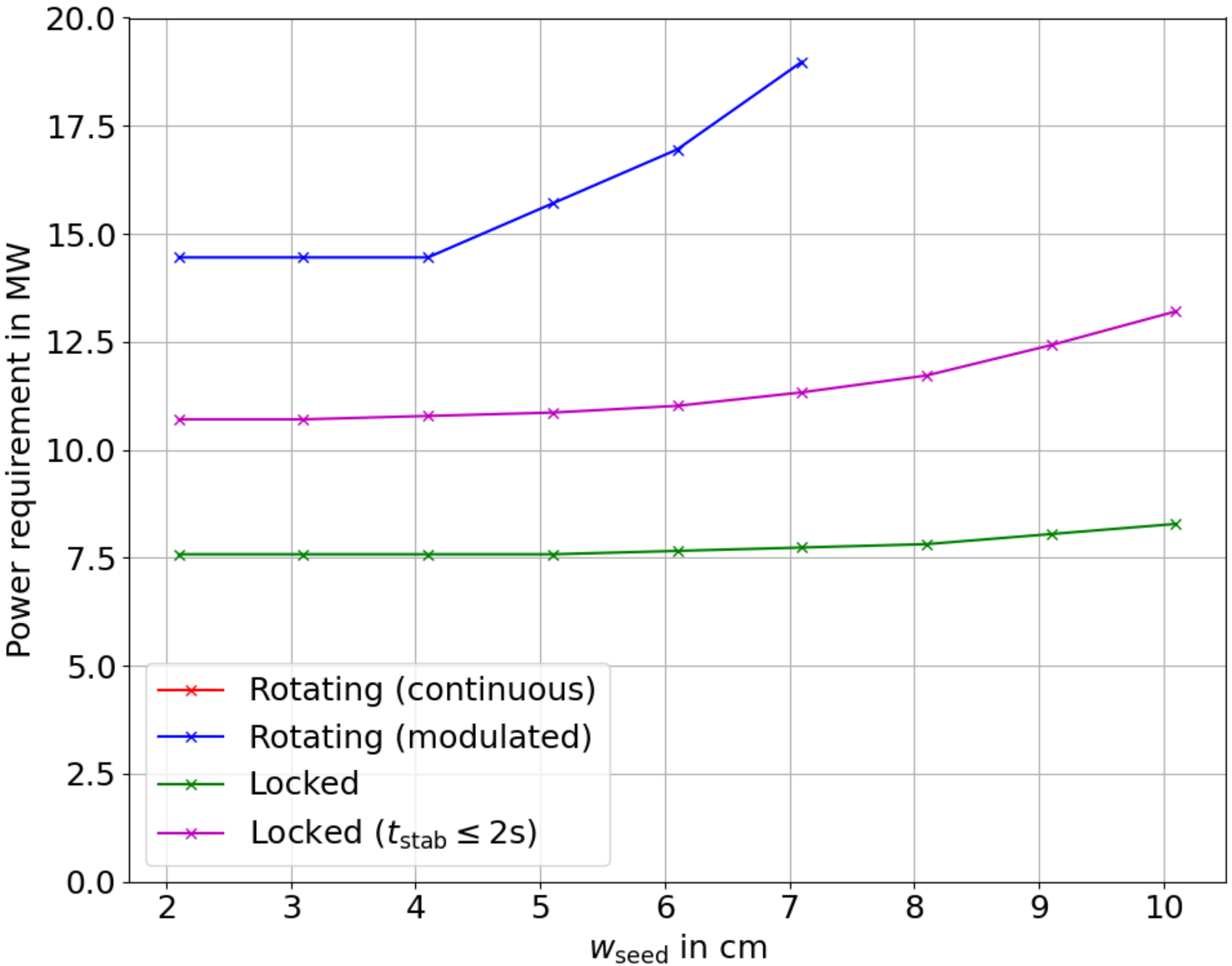

$w_{\mathrm{vac}} = 2.5$ cm

$w_{\mathrm{dep}} = 12$ cm

$x_{\mathrm{mis}} = 1$ cm

Criterion for rotating island:

$w < 4$ cm

Power requirement with higher x_{dep}

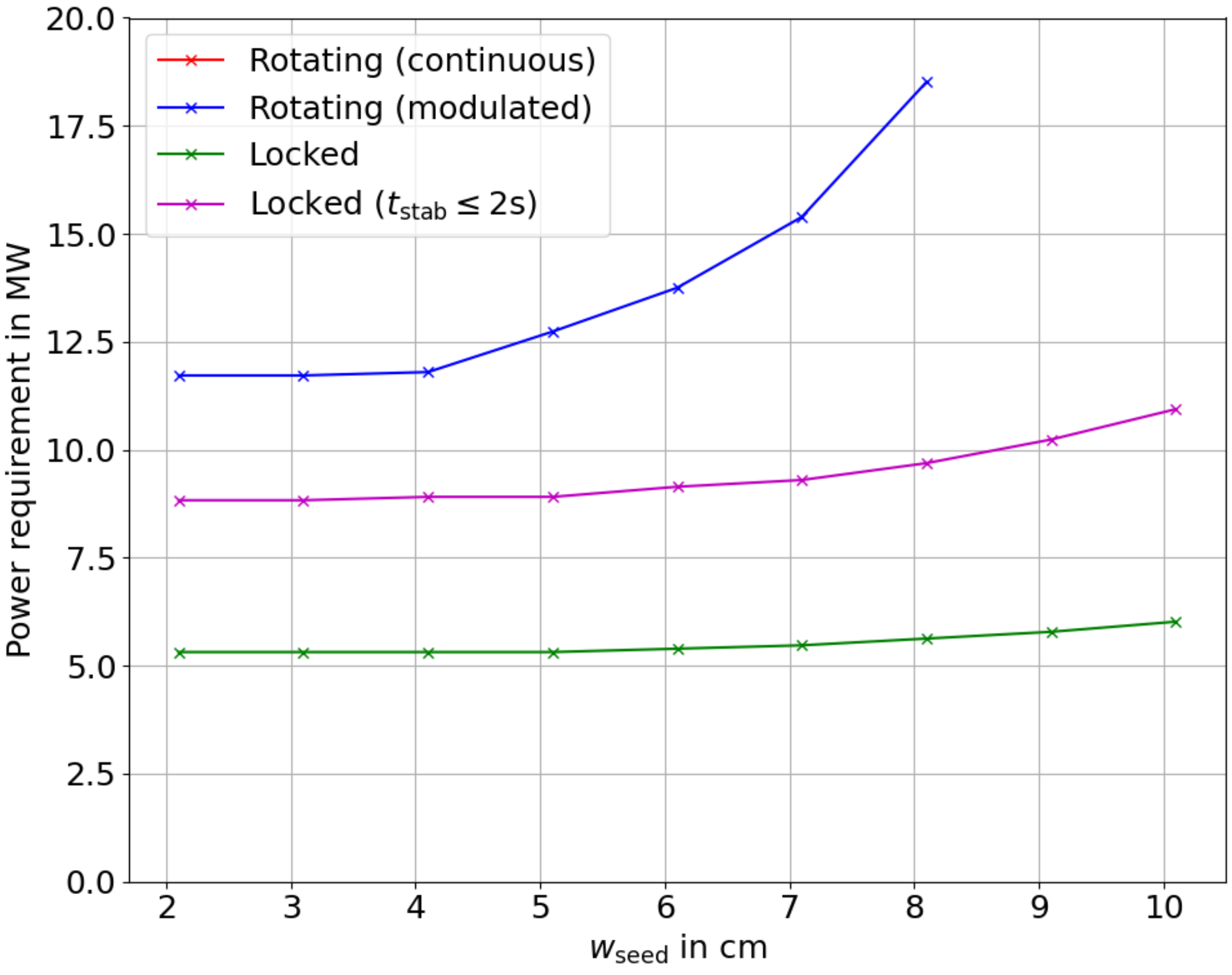

$w_{\mathrm{vac}} = 2.5$ cm

$w_{\mathrm{dep}} = 8$ cm

$x_{\mathrm{mis}} = 2$ cm

Criterion for rotating island:

$w < 4$ cm

Power requirement with combined stabilisation

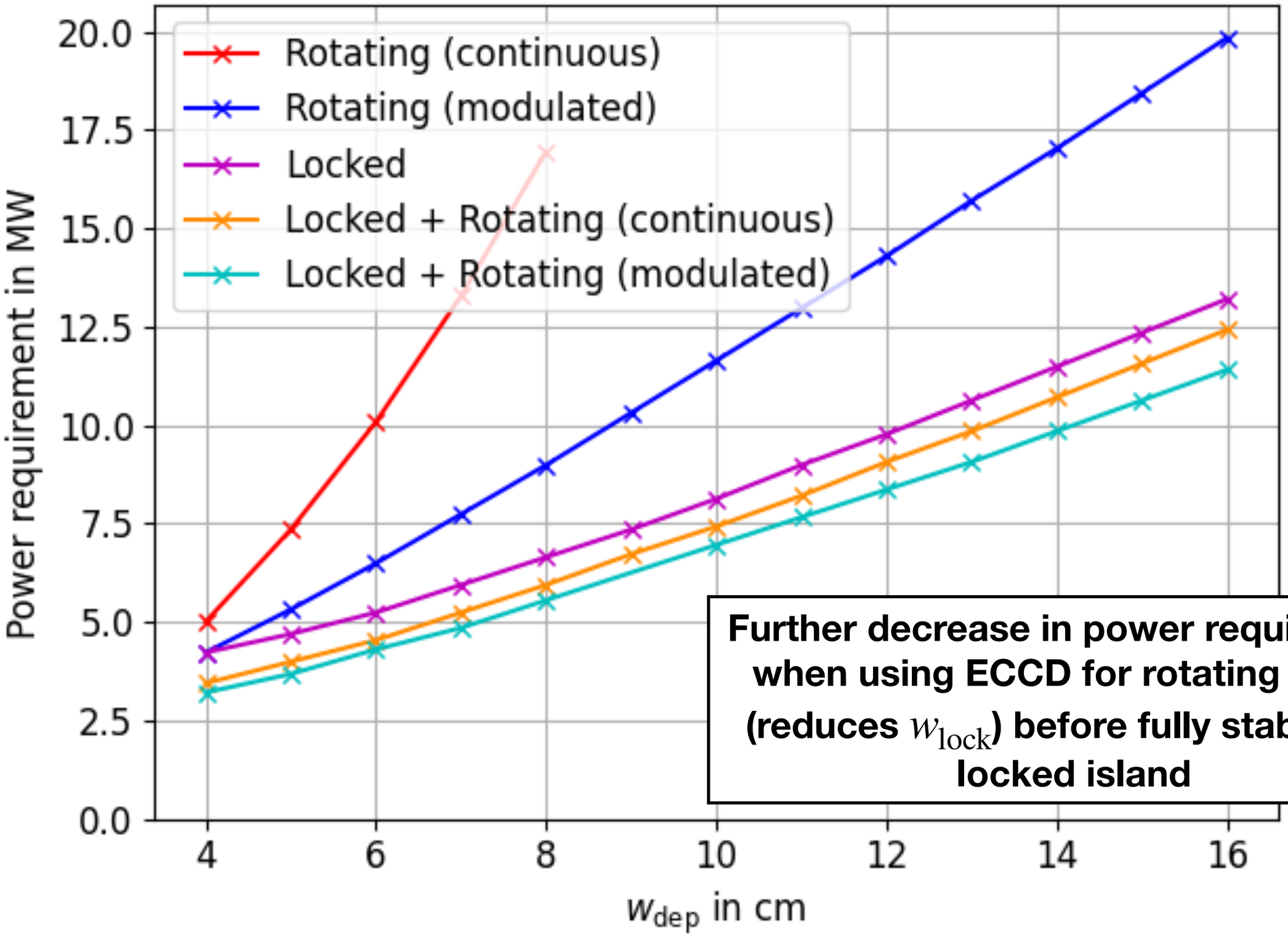

$w_{\mathrm{vac}} = 2.5$ cm

$w_{\mathrm{dep}} = 8$ cm

$x_{\mathrm{mis}} = 1$ cm

Criterion for rotating island: $w < 4$ cm

Further decrease in power requirement when using ECCD for rotating island (reduces w_{lock}) before fully stabilising locked island

Time delay / detection threshold

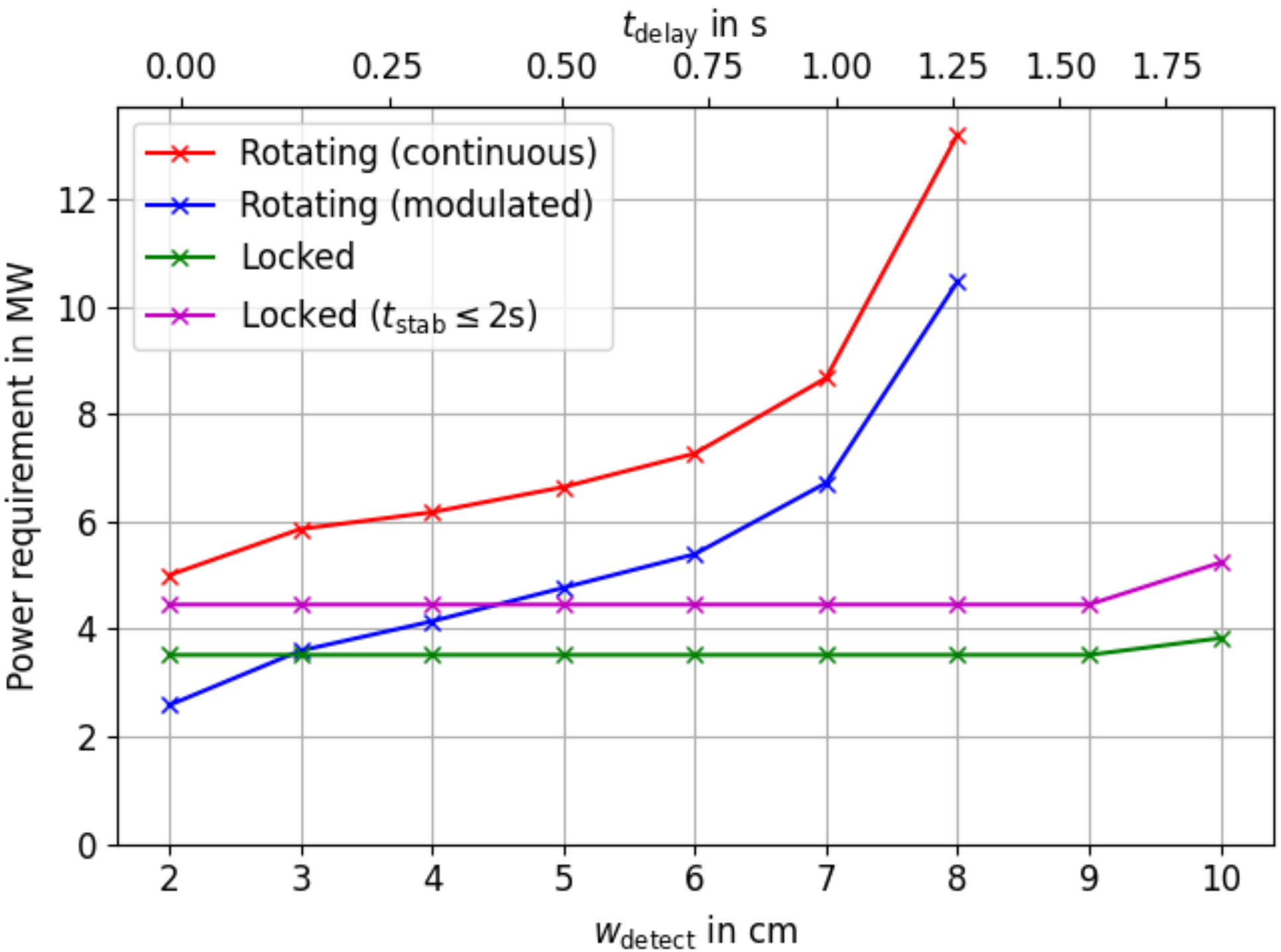

ECCD is turned on when $w > w_{\mathrm{detect}}$, **or** $t - t_{\mathrm{seed}} > t_{\mathrm{delay}}$.

The two can be combined, e.g.

$w_{\mathrm{detect}} = 4$ cm

$\Leftrightarrow t_{\mathrm{delay,det}} = 0.3$ s

and actual

$t_{\mathrm{delay,act}} = 0.5$ s.

Then, in plot,

$t_{\mathrm{delay}} = 0.8$ s

$\Leftrightarrow w_{\mathrm{detect}} = 6.25$ cm